

Lifetime estimation of coated articulating implants: accelerated testing to address crevice, stress and fatigue corrosion

E Ilic¹, A Pardo-Perez¹, R Hauert¹, P Schmutz¹, S Mischler²

¹ Empa, Swiss Federal Laboratories for Materials Science and Technology, Dübendorf, CH.

² EPFL, Tribology and Interfacial Chemistry Group, Lausanne, CH

INTRODUCTION: Diamond-like carbon (a-C:H) coatings are promising materials for improving the wear resistance of articulating biomedical implants due to their hardness and intrinsic durability. They can be applied directly onto the implant materials (TiAlNb, CoCrMo), but usually an adhesion promoting interlayer is used (Cr, Ti, Si, a-C:H-Si). However, coating delamination remains a problem due to crevice corrosion (CC) and stress corrosion cracking processes occurring at the interlayer/interface [1]. The aim of this study is to investigate and accelerate the localized corrosive degradation responsible for delamination at a coating-substrate interface, ultimately allowing for a more accurate predication of the Si or a-C:H-Si interlayer and implant coating lifetime.

METHODS: CC tests were carried out by clamping together Si wafer pieces and submerging for various durations in either 0.01 M phosphate buffered saline (PBS) or Hyclone (simulated joint fluid, with 30 g/L proteins) at temperatures ranging from 37 to 90 °C. For comparison, single Si wafer pieces were also submerged in each bulk solution.

RF-CVD has been used to deposit 4 µm a-C:H coatings using 90 to 250 nm a-C:H-Si interlayers on TiAlNb substrates. The interface composition with different oxygen contamination levels was analyzed by XPS depth profiles. The influence of alternating applied load on the interface stability was evaluated under dynamic loading of pre-damaged coatings via reciprocating sliding tests performed in PBS at 37 °C, using a 6 mm diameter alumina sphere.

RESULTS: Crevice corrosion susceptibility of Si: While no damage was observed on the single Si wafer pieces, crystallographic localized attacks (pits) and overall corroded depths of up to 3 µm were measured on the Si surfaces which had been clamped in crevice conditions, as seen in Fig. 1. Furthermore, the temperature dependent results yielded a linear Arrhenius relation with activation energies (E_a) of 106 kJ/mol in 0.01 M PBS, and 109 kJ/mol in Hyclone where active dissolution took place.

In a series of controlled oxygen contaminated deposition conditions, XPS analysis detected an enhanced oxide formation (SiO₂, TiO₂) with

increasing oxygen content exposure and parallel metal carbide reduction at the interface with the substrate.

In the reciprocal sliding test, the critical conditions of failure (load and frequency) have been determined both for a short time period (10⁴ Cycles), and under fatigue conditions (10⁶ Cycles).

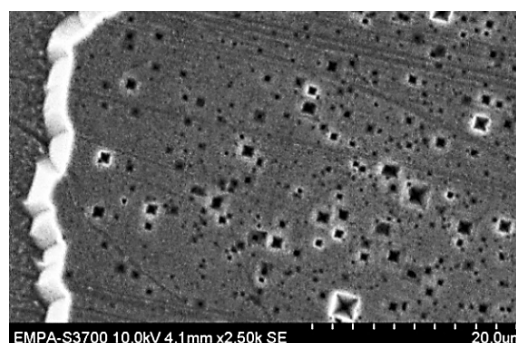


Fig. 1: SEM image of pits on Si surface after clamping against Si in Hyclone at 37 °C for 30 days.

DISCUSSION & CONCLUSIONS: The pits shown in Fig. 1 are characteristic of localized corrosion and etching and give strong indication that Si is vulnerable to crevice corrosion attack in physiological environments and should hence not be used as an interlayer material. Concerning the reciprocal sliding test, a comparison with the results in a replica coating tested in the spinal disk simulator [2], allows a fast and reliable test to predict the success of the in-vitro simulation. The methodology is applicable not only in the field of articulating implants but also to the general analysis of buried interlayers under dynamic load in media.

CC and corrosion fatigue susceptibility of interfaces and interlayers should be addressed in separate dedicated experiments to achieve reliable accelerated lifetime estimation of the articulating implants.

REFERENCES: ¹ R. Hauert et al (2013) *Surf Coat Technol* **233**:119. ² K. Thorwarth et al (2014) *Int. J. Mol. Sci.* **15**:10527

ACKNOWLEDGEMENTS: This work was supported by the Swiss National science foundation and Marie Heim-Vögtlin grant no. PMPDP2_171412.

Vascular imaging by novel contrast agent to advance preclinical models

N Warfving¹, R Hlushchuk², K Weber¹

¹ AnaPath Services GmbH, Liestal, CH. ² Institute of Anatomy, University of Bern, CH

INTRODUCTION: There is a growing interest in high-resolution imaging of vascular structures for different physiological or pathological challenges. Taking advantage of the available and widespread technology: high resolution micro computed tomography (microCT), a novel preclinical microvascular contrast agent allowing three-dimensional (3D) visualization and quantification of tissue vascularity. This combined technology provides high-resolution 3D imaging of microvasculature including the finest capillaries. Characterizing and quantifying vascularization and angiogenesis are important aspects of many preclinical models. Historically, such characterization of vascular abnormalities and angiogenesis involved either measurements made on two-dimensional tissue sections from 3D specimens, often with additional image analysis and immunohistochemistry, or measurements made on corrosion casts.

METHODS: Continuous advancements in spatial resolution, sub-micrometer, and decreasing scanning times for commercial microCT makes it a highly efficient technology for investigating strongly absorbing biological samples, such as bone, but fails in differentiating tissue with similar and weak X-ray absorption properties. To overcome the limitations of weak X-ray absorption in microCT several X-ray phase-contrast imaging techniques were recently developed. However, these methods often require sophisticated setups only to be found at large synchrotron facilities, which greatly limits the access to these technologies and its function as a technology for routine usage.

RESULTS: Radiopaque perfusion compounds, or contrast agents, used to enhance the contrast of low attenuating materials have become of high interest to researchers hoping to qualify therapeutic effects on the vasculature. Several different radiopaque substances like iodine, barium, and other metallic elements often in combination with a polymer can be injected to aid microCT imaging. A widely used preclinical contrast agent is composed of silicone rubber containing lead chromate. Nevertheless, challenges to overcome includes homogenous distribution of contrast agent throughout the

vasculature, perfusion and diffusion limitations, intensity of radiopaque and more. To the author's knowledge, previously no preclinical contrast agents have enabled visualization of the finest capillaries by commercial microCT technology. The novel contrast agent, μ Angiofil [1], has overcome these limitations and demonstrated visualization of even the finest capillaries (Fig. 1) in several tissues from both mice and rats including eye (Fig. 1), kidney, muscle and brain.

DISCUSSION & CONCLUSIONS: This new technology could greatly advance preclinical models and the understanding of many therapeutic effects such as accurate volume, quantity and distribution of glomerulus in renal drugs, induced effects on the vasculature from medical devices or quality control of angiogenesis in reconstructed and engineered tissue. The 3D vascular architecture in the brain is crucial to a range of neuropathological processes from dementia to stroke and Alzheimer's disease. Tumors are greatly dependent on vascularization for growth and assessment of microvasculature has become an important tool for studying angiogenesis and monitoring antiangiogenic therapies.

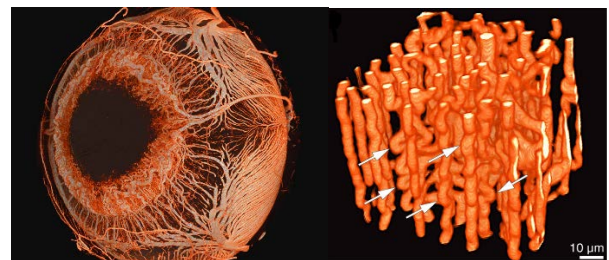


Fig. 1: 3D reconstruction from images of microCT scans showing an overview of a guinea pig eye and a high resolution scan displaying individual capillaries.

REFERENCES: ¹ L. Schaad, R. Hlushchuk, S. Barré, R. Gianni-Barrera, D. Haberthür, A. Banfi, V. Djonov (2017) Correlative Imaging of the Murine Hind Limb Vasculature and Muscle Tissue by MicroCT and Light Microscopy, *Scientific Reports* **7**: 41842, 1-12.

Thermal dissipation in active implantable medical devices for neuroengineering

JM Herrera-Morales

Wyss Center for Bio and Neuroengineering, Geneva, CH

INTRODUCTION: Active Implantable Medical Devices (AIMD) employed as Brain-Machine Interfaces (BMI) have the potential to benefit many patients affected by spinal cord injury or motor neuron diseases. Remarkable progress has been achieved in recent years by high-resolution cortical BMIs such as the BrainGate wireless neural interface tested in US clinical trials. Wyss Center for Bio and Neuroengineering has been working in collaboration with the inventors of this device to create a human grade AIMD approved by regulatory agencies in the US and Europe for treatment of neurological disorders. An important part of this endeavour is the mitigation of risks posed by the implanted device to user patients. One of the major challenges in this project is controlling the endogenous heat induced in the titanium canister by eddy currents during wireless power transfer. Consequently, thermal power dissipation in human tissues has been calculated and measured to comply with the FDA standard ISO 14708-1:2000 E that demands that no outer surface of implanted devices rise more than 2 °C above body temperature of 37 °C.

METHODS: Finite Element Methods (FEM) and benchtop measurements were performed to quantify heat generation. Our FEM model integrates different material properties and thickness for the scalp (7.5 mm), skull (5 mm) and brain surrounding the active implant, which lays on top of the brain, embedded by craniotomy in the skull and covered by scalp tissue. To quantify the rise in temperature of the tissue in contact with the AIMD, the standard bioheat transfer equation [1] (eq.1) was implemented in COMSOL Multiphysics 5.3 software (Stockholm, Sweden):

$$C\rho \frac{\partial T}{\partial t} = \nabla \cdot (k\nabla T) - Q_{per} + Q_{met} + Q_{ext} \quad (1)$$

where ρ is the tissue density ($\text{kg}\cdot\text{m}^{-3}$), C is its specific heat ($\text{J}\cdot(\text{kg}\cdot\text{K})^{-1}$), k is its thermal conductivity ($\text{W}\cdot(\text{m}\cdot\text{K})^{-1}$), Q_{per} is heat loss due to blood perfusion ($\text{W}\cdot\text{m}^{-3}$), and Q_{met} and Q_{ext} are heat sources arising from internal metabolism and external heating ($\text{W}\cdot\text{m}^{-3}$), respectively.

Out of 2 W of power transmitted wirelessly, 1.4 W are absorbed as eddy currents by the titanium case, which is a normal value for our AIMD [2].

RESULTS: Figure 1 shows a calculated thermal equilibrium as function of continuous power transfer and blood perfusion rate. FEM model results are summarised in Figure 2.

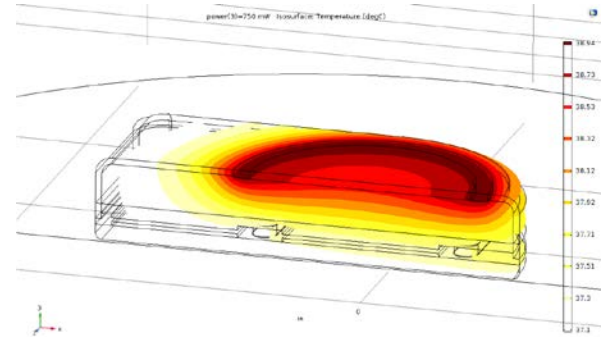


Fig. 1: Steady-state result obtained with 750 mW dissipated by eddy currents and blood perfusion rate of $3.6 \cdot 10^{-2} \text{ s}^{-1}$.

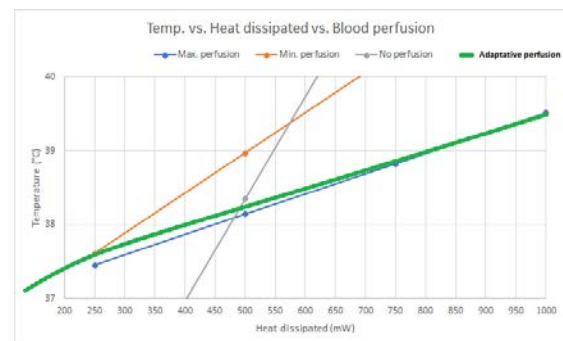


Fig. 2: Maximum temperature rise of tissue in contact with AIMD as function of heat dissipated and blood perfusion rate.

DISCUSSION & CONCLUSIONS: Thermal dissipation of AIMDs depends largely on blood perfusion rate. For neural devices, maximum heat dissipation is generally $6.7 [\text{mW}/(^\circ\text{C}\cdot\text{cm}^2)] * \text{Area}[\text{cm}^2] * \text{Temp}.[^\circ\text{C}]$, which yields 800 mW for a rise of 2 °C of tissue in contact with our device.

REFERENCES: ¹ P. D. Wolf (2008) *Indwelling Neural Implants: Strategies for Contending with the In Vivo Environment*, W. M. Reichert, Ed. Boca Raton (FL): CRC Press/Taylor & Francis. ² D. A. Borton, M. Yin, J. Aceros, and A. Nurmikko (2013) *Journal of Neural Engineering* **10-2**:026010.

ACKNOWLEDGEMENTS: We thank Brown University and Arto Nurmikko for their collaborative role in this project.

Future lubrication of dry and wet contacts

[CH Mathis](#), [O Sterner](#), [S Zürcher](#), [SGP Tosatti](#)

[SuSoS AG](#), Dübendorf, CH

INTRODUCTION: Medical devices and instruments frequently depend on tribological performance of one or multiple parts therein. Classical solutions like siliconization or hydrophilic coatings have limitations and industry demands a new solution. While siliconization can serve to reduce dry friction, uncontrolled detachment of molecules has rendered siliconization unsuitable for delicate applications, such as in the field of ophthalmology [1,2]. Hydrophilic coatings on the other hand slide perfectly, however requiring an aqueous fluid to be present.

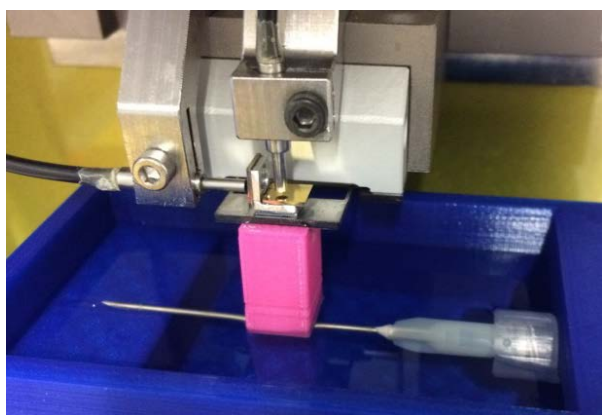


Fig. 1: Experimental setup for evaluating the frictional properties of needle coatings in both dry and wet conditions.

METHODS: SuSoS' newest development, the AziGrip4™ WD coating, turns tribological contacts into low friction surfaces under both dry and wet conditions. It does so by combining a hydrophilic functionality as well as a confined dry lubricant. For individual optimization, the coating can be adjusted to comply with a wide range of commercially used medical grade lubricants. Depending on the requirements, structural properties are tuneable to operate under harsh tribological conditions and provide lubrication in alternating dry and wet conditions. Evaluation of the friction performance can be obtained for example through measuring the frictional forces arising, when sliding along a coated or uncoated injection needle surface, as shown in Figure 1 above. To illustrate the effect of the AziGrip4™ WD coating in both dry and wet conditions in comparison with existing industrial coatings, respectively coated needles were tested using a microtribometer setup.

RESULTS: The friction force measured during sliding in reciprocal motion along the needle surface was measured for classically siliconized needles and needles coated with the new AziGrip4™ WD coating. The needles were tested both in dry conditions as well as after addition of water after 10 sliding cycles. From Figure 2 it is apparent that AziGrip4™ WD coatings provide a very low coefficient of friction compared to the siliconized coatings. In the dry case, controlled wear can occur dependent on the viscosity of the lubricant confined in the AziGrip4™ WD coating. Under wet conditions the low friction performance endures throughout the testing duration.

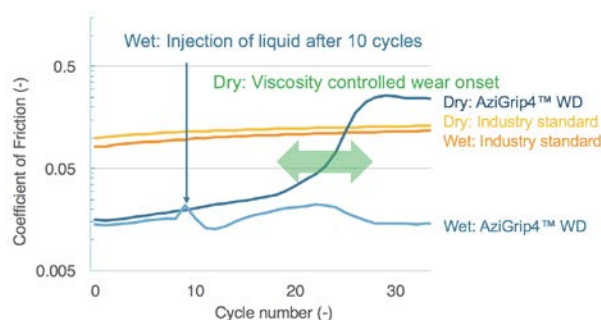


Fig. 2: Coefficient of friction of an injection needle coated with AziGrip4™ WD.

DISCUSSION & CONCLUSIONS: Using the example of an injection needle application, we demonstrate how next generation medical devices are enabled to meet the demands of miniaturization and to deliver optimal patient comfort. We illustrate the path from transitioning off existing technologies all the way to implementing the new coating solution to advance next generation medical devices.

REFERENCES: ¹ E. Krayukhina, K. Tsumoto, S. Uchiyama and K. Fukui (2015) *J. Pharm. Sci.* **104**:527-35. ² F. Felsovalyi, S. Janvier, S. Jouffray, H. Soukiassian and P. Mangiagalli (2012) *J. Pharm. Sci.* **101**:4569-83.

Laser based microtomy for advanced histology of hard tissue and implanted tissue

H Richter, I Bleeker, D Ramirez, F Will, B Stolze

LLS ROWIAK LaserLabSolutions GmbH, Hannover, Germany

INTRODUCTION: Preclinical studies in the field of regenerative medicine become more and more important due to regulatory requirements and to competitiveness in the market. Histological analysis often is a mandatory, yet laborious part of preclinical study design. Laser microtomy is a novel method for fast and easy preparation of histology sections of hard tissue and tissue containing implants or biomaterials. In this contribution we demonstrate that laser based microtomy of resin embedded tissue enables for applying a broad range of classical histological stainings and may also be suitable for advanced histochemical and immunohistochemical analysis.

METHODS: Different types of hard tissue (e.g. bone, cochlea, jaw) or tissue containing implants (e.g. stented vessels, fixing screws) were embedded. Hard tissue was not subject to prior decalcification. Nearly serial sections were prepared by laser microtomy at ~10 µm thickness. Histological, histochemical and immunohistochemical stainings were applied as indicated in the results.

RESULTS: The histological slide preparations show that routine stainings can be successfully applied to thin sections performed by laser microtomy as shown by SRS/van Gieson, McNeal or Masson Goldner staining (Fig. 1). The sections show tissue architecture and cellular details clearly. Special detection of enzyme activity inside bone samples was demonstrated by Tartrate-Resistant Acid Phosphatase (TRAP) staining of osteoclasts after laser microtomy (Fig. 2), implicating that the laser cutting did not destroy the enzymes. Immunohistochemistry was performed for antigens as SMA (Fig. 2), Col-I or CD31 (not shown).

DISCUSSION & CONCLUSIONS: Femtosecond laser based tissue sectioning opens a new range of possibilities for histological analysis of hard undecalcified or implanted tissues. A range of histological stains, even trichrome stains, can be routinely applied with high quality to plastic embedded samples. The results indicate that thin sections prepared by laser microtomy can be applied to histochemistry or immunohistochemistry and that main enzymes or antigens are not impaired by laser sectioning.

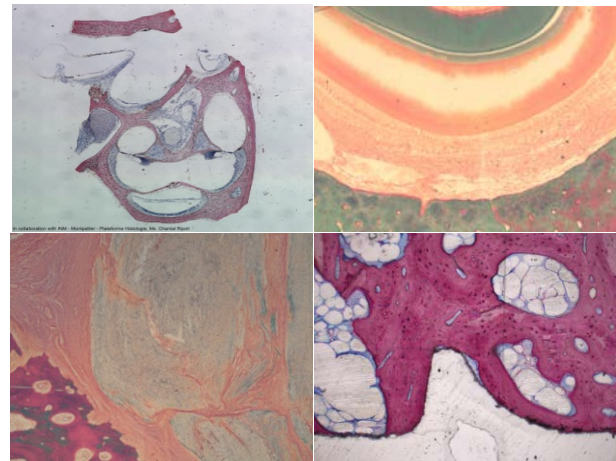


Fig. 1: Histochemical stainings of undecalcified hard tissue: Mouse cochlea stained SRS/van Gieson (upper left), Masson Goldner Trichrome stain of mouse jaw (upper right) and of rat femur with polymer implant (lower left), McNeal stain of bone section from screw implant (lower right).

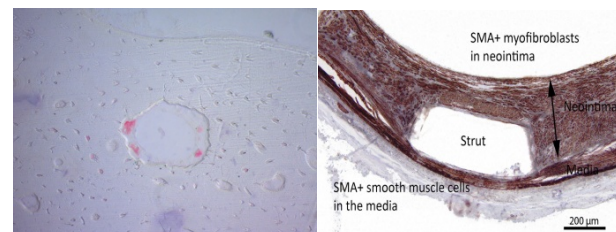


Fig. 2: Enzyme Histochemistry and immunohistochemistry: TRAP staining of mouse femur osteoclasts (left), SMA immunohistochemistry in neointima of stented pig artery (right).

REFERENCES: ¹ H. Richter, et al (2015) Time- and material saving laser microtomy for hard tissue and implants. *European Cells and Materials* **29**: Suppl.2, p 4. ² A. Boyde, et al (2017) A distinctive patchy osteomalacia characterises Phospho1 deficient mice. *J. Anat.* **231**:298-308. ³ A.-M. Pobloth, et al (2018) Mechanobiologically optimized 3D titanium-mesh scaffolds enhance bone regeneration in critical segmental defects in sheep. *Sci Transl Med* **10**: eaam 8828.

ACKNOWLEDGEMENTS: We thank Prof. B. Müller-Hilke (Institute of Immunology, Rostock) and Alizee Pathology for providing samples and pictures for TRAP and IHC.

Surface improvement of PEEK by Multicharge Ion Implantation

M Dadrás¹, O Sereda¹, A Bohlen¹, K Vaideeswaran¹, C Yamahata²

¹ CSEM, Neuchâtel, CH.

² Idonus Sarl, Hauterive, CH

INTRODUCTION: Biocompatible materials are extremely surface sensitive, with their interactions with the environment being heavily influenced by their surface properties. However, the high dose ion implantation of polymers is of great interest for future biocompatible applications in the medicine field. Influence of ion implantation was studied by different researcher [1, 2] but the influence of Multicharge Ion Implantation (MCII) on tribology properties remains to be clarified.

The main objective of this study is to improve the tribological properties of biocompatible materials, specifically polyetheretherketone (PEEK), by MCII using helium ions.

METHODS: An extruded PEEK rod was He implanted using an Electron Cyclotron Resonator (ECR). SRIM Software was used for estimation of the penetration depth for the Helium ions. For a dose of $0.1 \cdot 10^{16}$ ions/cm² accelerated at 20 kV, the maximum concentration of ions was calculated to be around ~280 nm from the surface with a full width half maximum (FWHM) of ~130 nm. ECR technology permits simultaneously implantation of He having different charges (He⁺, He²⁺). Tribology properties as Coefficient of Friction (CoF) and wear was measured using a CSM Instruments Nanotribometer. The applied load, sliding velocity and sliding distance were 5 mN, 0.5 cm/s and 40 m, respectively. The applied loads were limited to 5 mN, corresponding to expected values of contact pressure in implant applications (~10 MPa). The profile of the wear tracks was measured by the WYKO Rough Surface Tester (RST) Light Interferometer.

RESULTS: Figure 1 presents the wear rate of samples before and after implantation with different doses and energies.

The wear decreased from $1.6 \cdot 10^{14}$ m²/N to near $2 \cdot 10^{15}$ m²/N for reference sample and implanted one. Figure 2 shows the surface wear after tribology tests in the case of reference and implanted samples. Nearly no wear trace is observed in the implanted sample.

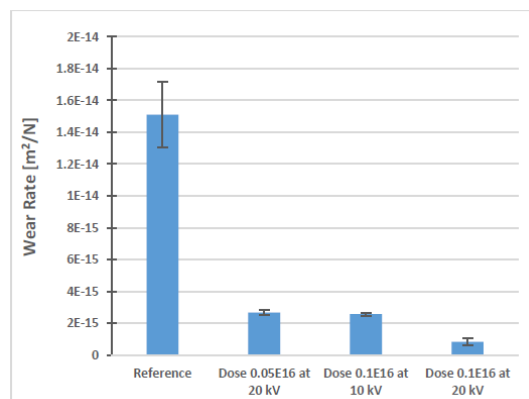


Fig. 1: Wear Rate of PEEK before implantation (reference) and after He ion implantation.

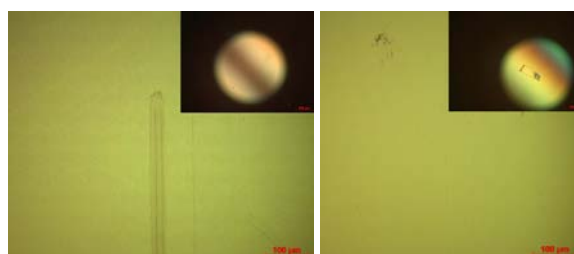


Figure 2: For sliding distance of 40 m (at 5 mN), the reference PEEK surface (left) shows a clear sliding trace on the surface. The implanted sample at $0.1 \cdot 10^{16}$ ions/cm² at 20 kV (right) shows nearly no trace. The surface of the steel ball (shown in insets) shows no wear for the reference sample, while for all the implanted surfaces a clear wear of the steel ball is observed.

CONCLUSION:

The study showed that the surface properties of the PEEK can be improved and that a wear resistant surface layer can be formed by helium ion implantation at very low energy.

REFERENCES: ¹ A. Macková, V. Havránek, V. Švorčík, N. Djourelov, T. Suzuki (2005) Degradation of PET, PEEK and PI induced by irradiation with 150 keV Ar⁺ and 1.76 MeV He⁺ ions in *Nuclear Instruments and Methods in Physics Research B* **240**:245–249. ² M. Niklaus, S. Rosset, M. Dadrás, P. Dubois, H. Shea (2008) Microstructure of 5 keV gold-implanted polydimethylsiloxane in *Scripta Materialia* **59**:893–896.